

UC Berkeley
SEMM Reports Series

Title

A Perturbed Lagrangian Formulation for the Finite Element Solution of Contact Problems

Permalink

<https://escholarship.org/uc/item/1tf7t9s4>

Authors

Simo, Juan

Wriggers, Peter

Taylor, Robert

Publication Date

1984-08-01

A Perturbed Lagrangian Formulation for the Finite Element Solution of Contact Problems

Juan C. Simo † Peter Wriggers * Robert L. Taylor

Department of Civil Engineering, University of California, Berkeley.

Abstract

Making use of a perturbed Lagrangian formulation, a finite element procedure for contact problems is developed for the general case in which node-to-node contact no longer holds. The proposed procedure leads naturally to a discretization of the contact interface into *contact segments*. Within the context of a bilinear interpolation for the displacement field, a mixed finite element approximation is introduced by assuming *discontinuous* contact pressure, *constant* on the contact segment. Because of this piece-wise constant approximation, the gap function enters into the formulation in an "average" sense instead of through a point-wise definition. Numerical examples are presented that illustrate the performance of the proposed procedure.

Contents

1. Introduction.
 2. Perturbed Lagrangian Formulation.
 - 2.1. Contact Kinematics.
 - 2.2. Variational Formulation.
 3. Mixed Finite Element Formulation.
 - 3.1. Kinematics of the Slide Line.
 - 3.2. Interpolation within a Contact Segment.
 - 3.3. Finite Element Approximation.
 4. Penalty Procedure via Perturbed Lagrangian.
 5. Numerical Examples.
 6. Concluding Remarks.
- References.

August 3, 1984

EARTHQUAKE ENG. RES. CTR. LIBRARY
Univ. of Calif. - 453 R.F.S.
1301 So. 46th St.
Richmond, CA 94804-4698 USA
(510) 231-9403

A Perturbed Lagrangian Formulation for the Finite Element Solution of Contact Problems

Juan C. Simo † Peter Wriggers * Robert L. Taylor

Department of Civil Engineering, University of California, Berkeley.

1. Introduction

Current finite element formulations for contact problems based on either the classical Lagrange parameter procedure [1,2,3,12,20] or the penalty function method [4,5,6,11], are characterized by a point-wise enforcement of the contact constraint condition, in the sense that penetration of the bodies is established on a nodal basis. Moreover, in this methods the recovery of the contact pressure over the element from the contact nodal forces generally requires an additional procedure. Within the framework of classical Lagrange multiplier methods the contact condition is exactly satisfied by transforming the constrained problem into an unconstrained one with the introduction of additional variables (Lagrange multipliers). These extra variables add computational effort to the solution process which often requires special procedures to handle the presence of zero diagonal terms. Penalty methods, on the other hand, enable one to transform the constrained problem into an unconstrained one without introducing additional variables. The constraint condition is now satisfied only approximately for finite values of the penalty parameter. The main difficulty associated with these methods, however, lies in the poor conditioning of the problem as the penalty is increased to more accurately enforce the constraint condition. This is a well understood phenomenon, particularly in the context of the incompressible and nearly incompressible problem in solid and fluid mechanics (e.g. see [15,22,25] for a review). Recently, augmented Lagrangian procedures have been proposed as a promising way to partially overcome these difficulties and "regularize" the penalty formulation (e.g. see the survey in [7] and [8]).

Within the framework of *linearized kinematics*, it is possible to restrict the finite element formulation of contact problems by assuming that node-to-node contact occurs. This is in fact the case often considered in the literature [1,2,4,6,12,20,21]. In the general context of fully nonlinear kinematics, however, it is no longer possible to place such a restrictive assumption on the formulation. Several schemes have been devised, particularly from the computational side [5,11], which are capable of enforcing the contact conditions in the general situation for which node-to-node contact does not hold. In this paper, a novel approach for the enforcement of the contact constraint in this general context is presented, based on a *perturbed* Lagrangian formulation. We recall that the perturbed Lagrangian is obtained from the classical Lagrangian functional by *regularization* with a *quadratic* (positive) term in the Lagrange multiplier vector (e.g., see [15] Sec 3.2, and [22]).

† Post-Doctoral Fellow

* Visiting Scholar. Institut fuer Baumechanik und numerische Mechanik, Universität Hannover

Our formulation may be summarized as follows. On the basis of the perturbed Lagrangian formulation of the contact problem, a mixed finite element approximation is introduced in which the contact pressure is independently approximated over the contact interface. Such an approach requires a special treatment of the contact surface, now viewed as an assembly of contact segments which are unambiguously defined for the general situation where node-to-node contact does no longer hold. As in the treatment of the incompressibility constraint several approximation schemes are possible within the context of a perturbed Lagrangian formulation (e.g. see [15,22 Chap. 3,25]). Confining our attention to the case of a bi-linear isoparametric interpolation for the displacement field, it is assumed that the contact pressure is *constant* on each contact segment. As a result of this piece-wise constant approximation of the contact pressure, *discontinuous across contact segments*, the contact constraint is enforced in an "average" sense on each contact segment. In effect, the *average* gap over a contact segment is the crucial kinematic variable on the basis of which penetration between the two bodies is established.

The formulation advocated in this paper is intended for the general case of fully nonlinear kinematics, although for simplicity in the presentation attention is restricted to the linear case. This approach is applicable to contact problems involving two deformable bodies, as well as problems involving a deformable body subjected to unilateral constraints. Furthermore, although the contact pressure does not enter into the formulation explicitly it can be consistently recovered via the augmented Lagrangian procedure.

The numerical examples presented in Section 5. are intended to demonstrate the differences in performance of the procedure advocated here relative to established nodal penalty methods.

2. Perturbed Lagrangian Formulation

In this section we develop the variational equations governing the contact problem with *linearized kinematics*, based on the use of a perturbed Lagrangian procedure. First, we briefly summarize some kinematic relations which are necessary for the description of the contact constraint condition. For simplicity, we shall confine our attention to the case of linear kinematics, leaving the consideration of the finite deformation situation to a forthcoming paper. In addition, we restrict ourselves to frictionless contact problems throughout the developments that follows.

2.1. Contact Kinematics. Consider two bodies with initial configurations denoted by Ω^1 , $\Omega^2 \subset \mathbb{R}^3$, and displacement fields given by

$$\mathbf{u}^1 = \hat{\mathbf{u}}^1(\mathbf{x}^1), \quad \mathbf{x}^1 \in \Omega^1; \quad \mathbf{u}^2 = \hat{\mathbf{u}}^2(\mathbf{x}^2), \quad \mathbf{x}^2 \in \Omega^2. \quad (2.1)$$

Further, assume that the bodies are in contact along a surface γ^c with unit normal field $\mathbf{n}(\mathbf{x})$. This contact surface -not known in advance- may be characterized as follows. One assumes that there are parts of the boundary $\partial_c \Omega^1$ and $\partial_c \Omega^2$ in the initial configurations Ω^1 and Ω^2 of the two bodies, which may be defined *a priori*, so that their images contain the contact surface; that is,

$$\gamma^c \equiv \hat{\mathbf{u}}^1(\partial_c \Omega^1) \cap \hat{\mathbf{u}}^2(\partial_c \Omega^2). \quad (2.2)$$

The normal vector field to γ^c is given by

$$\mathbf{n} = \nabla \gamma^c(\mathbf{x}) / \|\nabla \gamma^c(\mathbf{x})\|. \quad (2.3)$$

Let \mathbf{t}^1 and \mathbf{t}^2 be the traction vectors acting on the boundaries $\hat{\mathbf{u}}^1(\partial_c \Omega^1)$ and $\hat{\mathbf{u}}^2(\partial_c \Omega^2)$ of the bodies in contact through the surface γ^c . Further, let $g_0(\mathbf{x})$ be the initial gap between the two bodies. Then, the local form of the contact condition may be formulated as follows

$$g \equiv [\mathbf{u}^2 - \mathbf{u}^1] \cdot \mathbf{n} + g_0 \geq 0, \quad \text{and} \quad \mathbf{t}^1 \cdot \mathbf{n} \equiv -\mathbf{t}^2 \cdot \mathbf{n} \leq 0, \quad \text{on } \gamma^c, \quad (2.4a)$$

where g gives the current value of the gap. The *current gap* and the contact force are related through the inequality conditions

$$\begin{cases} [\mathbf{u}^2 - \mathbf{u}^1] \cdot \mathbf{n} + g_0 = 0 & \Rightarrow & \mathbf{t}^1 \cdot \mathbf{n} \equiv -\mathbf{t}^2 \cdot \mathbf{n} < 0 \\ [\mathbf{u}^2 - \mathbf{u}^1] \cdot \mathbf{n} + g_0 > 0 & \Rightarrow & \mathbf{t}^1 \cdot \mathbf{n} \equiv -\mathbf{t}^2 \cdot \mathbf{n} = 0 \end{cases} \quad (2.4b)$$

Introducing the notation $\lambda = \mathbf{t}^1 \cdot \mathbf{n} \equiv -\mathbf{t}^2 \cdot \mathbf{n}$ for the *contact force* acting on γ^c , the contact conditions (2.4a,b) may be expressed in the following equivalent (Kuhn-Tucker) form

$$g\lambda = 0, \quad \lambda \leq 0, \quad g \geq 0, \quad \text{on } \gamma^c. \quad (2.5)$$

The form (2.5) of the contact condition is best suited for applications and immediately leads to a variational formulation in terms of Lagrange parameters. By a slight abuse in notation we shall employ again the same symbol λ for the Lagrange parameter.

Remark 2.1. The spaces of *kinematically admissible* variations or test functions for the problem at hand are defined as

$$V^A = \{ \boldsymbol{\eta}^A: \hat{\mathbf{u}}^A(\Omega^A) \rightarrow \mathbb{R}^3 \mid \boldsymbol{\eta}^A|_{\partial_u \Omega^A} = \mathbf{0} \}, \quad (A=1,2), \quad (2.6)$$

where $\partial_u \Omega^A$ is the part of the boundary with prescribed displacements $\hat{\mathbf{u}}^A|_{\partial_u \Omega^A} = \bar{\mathbf{u}}^A$. Typically, an appropriate choice for V^A is $H^1(\Omega^A)$, see e.g., [23, Chap.5]. Note that V^A , ($A=1,2$) are *unconstrained* configuration spaces which must be further restricted to account for the contact constraint. The Lagrangian formulation discussed below avoids the introduction of this constraint and enables one to work directly with the unrestricted spaces V^A as defined in (2.6). \square

2.2. Perturbed Lagrangian Formulation. Throughout this section we consider the case of an elastic material with stored energy function given by $W(\mathbf{x}, \nabla^S \mathbf{u})$, where a superposed S indicates the symmetric part. Ignoring for the moment the interaction between bodies, the total potential energy associated with each body in its final configuration $\mathbf{u}^A = \hat{\mathbf{u}}^A(\mathbf{x}^A)$ is given by

$$\bar{\Pi}^A(\hat{\mathbf{u}}^A) \equiv \int_{\Omega^A} W \, dv - \int_{\Omega^A} \rho \mathbf{b}^A \cdot \mathbf{u}^A \, dv - \int_{\partial_\sigma \Omega^A} \bar{\mathbf{t}}^A \cdot \mathbf{u}^A \, da, \quad (A=1,2), \quad (2.7)$$

where \mathbf{b}^A is the body force, $\bar{\mathbf{t}}^A$ is the surface traction specified on the part of the boundary $\partial_\sigma \Omega^A$, and ρ is the density. One of course requires that $\gamma^c \cap \partial_\sigma \Omega^A = \emptyset$ ($A=1,2$).

In order to build the contact constraint (2.5) into a variational formulation without restricting the spaces of kinematically admissible variations V^A , we introduce a Lagrangian functional $\Pi_\epsilon(\hat{\mathbf{u}}^1, \hat{\mathbf{u}}^2, \lambda)$, depending on a positive parameter $\epsilon > 0$, and defined by expression

$$\Pi_\epsilon(\hat{\mathbf{u}}^1, \hat{\mathbf{u}}^2, \lambda) \equiv \sum_{A=1}^2 \bar{\Pi}^A(\hat{\mathbf{u}}^A) + \int_{\gamma^c} \lambda \{[\mathbf{u}^2 - \mathbf{u}^1] \cdot \mathbf{n} + g_0\} da - \frac{1}{2\epsilon} \int_{\gamma^c} \lambda^2 da. \quad (2.8)$$

The last term in (2.8) depending on ϵ has the form of a *penalty* term and serves the purpose of *regularizing* the classical Lagrangian. One refers to the functional $\Pi_\epsilon(\hat{\mathbf{u}}^1, \hat{\mathbf{u}}^2, \lambda)$ as an *perturbed Lagrangian*, and expects that as $\epsilon \rightarrow \infty$ the solution obtained from (2.8) will converge (in the sense of weak convergence) to the solution obtained by the classical Lagrange multiplier method. For a discussion of this and related questions in the context of *linear* problems, we refer to [15].

Remark 2.2. The stiffness matrix for the discrete problem arising from the classical Lagrangian multiplier method always contains *zero diagonal terms*. The solution of the algebraic problem often requires special strategies, particularly in the three dimensional situation. From a computational standpoint the addition to the Lagrangian of the "penalty term" depending on ϵ , leads to positive definite stiffness matrices for the discrete problem with *non-zero* diagonal terms. \square

For each $\epsilon > 0$, the equilibrium configurations and corresponding contact pressures, $(\hat{\mathbf{u}}_\epsilon^1, \hat{\mathbf{u}}_\epsilon^2, \lambda_\epsilon)$, are characterized by rendering the perturbed Lagrangian $\Pi_\epsilon(\hat{\mathbf{u}}_\epsilon^1, \hat{\mathbf{u}}_\epsilon^2, \lambda_\epsilon)$ *stationary*. Accordingly, at $(\hat{\mathbf{u}}_\epsilon^1, \hat{\mathbf{u}}_\epsilon^2, \lambda_\epsilon)$ the following conditions must hold

$$D_A \Pi_\epsilon \cdot \boldsymbol{\eta}^A \equiv \left. \frac{d}{d\xi} \Pi_\epsilon(\hat{\mathbf{u}}_\epsilon^A + \xi \boldsymbol{\eta}^A, \lambda_\epsilon) \right|_{\xi=0} = 0, \quad (A=1,2) \quad (2.9)$$

$$D_\lambda \Pi_\epsilon q \equiv \left. \frac{d}{d\xi} \Pi_\epsilon(\hat{\mathbf{u}}_\epsilon^A, \lambda_\epsilon + \xi q) \right|_{\xi=0} = 0. \quad (2.10)$$

From conditions (2.9) and (2.10) and the expression (2.8) for Π_ϵ , one obtains the following two variational equations which form the basis of the mixed finite element approximation discussed in this paper

$$G_1 \equiv \sum_{A=1}^2 D_A \bar{\Pi}^A \cdot \boldsymbol{\eta}^A + \int_{\gamma^c} \lambda_\epsilon [\boldsymbol{\eta}^2 - \boldsymbol{\eta}^1] \cdot \mathbf{n} da = 0 \quad (2.11a)$$

$$G_2 \equiv \int_{\gamma^c} q \left[-\frac{\lambda_\epsilon}{\epsilon} + [\hat{\mathbf{u}}_\epsilon^2 - \hat{\mathbf{u}}_\epsilon^1] \cdot \mathbf{n} + g_0 \right] da = 0 \quad (2.11b)$$

In what follows, for notational simplicity we shall drop the subscript ϵ in λ_ϵ and $\hat{\mathbf{u}}_\epsilon^A$.

3. Mixed Finite Element Formulation.

In this section we consider a mixed finite element formulation for the numerical solution of the class of contact problems outlined in Sect. 2, based on the variational equations (2.11). To this end, we first examine some basic kinematic notions involved in the approximation of a typical slideline (i.e., contact surface). An essential feature that characterizes the approach proposed herein is the use of an "intermediate" contact surface which arises naturally from our discretization of the contact interface into "contact segments", as illustrated in Fig. 3.1.

For simplicity, throughout the present development attention is focussed on the 4-node isoparametric element. The proposed mixed finite element approximation based on equations

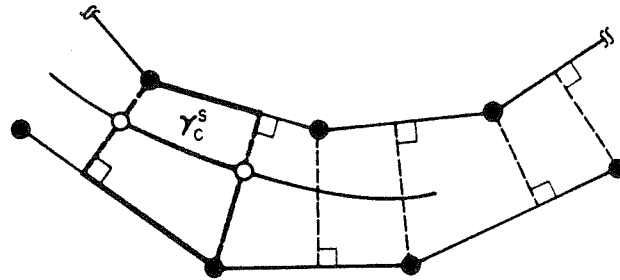


FIG. 3.1 DISCRETIZATION OF THE CONTACT INTERFACE INTO "CONTACT SEGMENTS."

(2.11) will then be characterized by assuming *constant* contact pressures on each segment of the interpolated slideline.

3.1. Kinematics of the Slide Line: Intermediate Contact Surface. During the deformation process, the two bodies Ω^1 and Ω^2 under consideration come into contact along the surface γ^c which for the *continuum* problem is defined by (2.2). Consider now a standard finite element discretization of the bodies Ω^A defined as

$$\bar{\Omega}^A \approx \bigcup_{i=1}^{E_A} \bar{\Omega}_i^A, \quad \Omega_i^A \cap \Omega_j^A = \emptyset, \quad i \neq j \quad (A=1,2) \quad (3.1)$$

As a result of this discretization, the parts of the boundary $\partial\Omega_c^1$ and $\partial\Omega_c^2$ which according to (2.2) contain γ^c , are replaced by polygonal approximations in which the vertices are nodal points. Further, due to the numerical formulation of the the contact conditions involving a penalty term, conditions (2.4) do not exactly hold and penetration of one body into the other necessarily occurs. The question then arises as to how the contact interface and its corresponding normal field may be unambiguously characterized. A procedure often employed is to arbitrarily select either one of the surfaces $\partial\Omega_c^1$ or $\partial\Omega_c^2$ as contact surface. This surface is often referred to as master surface. The choice of master surface is apparent in the case of unilateral (rigid) constraints or when one of the bodies in contact is much stiffer than the others. For cases in which the bodies in contact possess similar stiffness, the choice is no longer obvious and may indeed bias the results. These difficulties have motivated the use of "symmetric treatments" of the slideline such as the ones advocated in [5,11]. The procedure proposed herein, on the other hand, replaces the notion of master surface by the intermediate contact surface.

Geometry of a typical contact segment. The description of the slideline that characterizes the procedure proposed herein is illustrated in Fig 3.1, where a possible general discretization of the contact interface is shown. As indicated in Fig. 3.1, the contact interface is divided into *contact* segments which will allow a smooth definition of the gap function. A typical contact segment, shown in Fig 3.2, is defined as follows.

Consider two adjacent elements in the slideline with straight edges defined by their nodes $\mathbf{x}_2^1 - \mathbf{x}_1^1$ and $\mathbf{x}_2^2 - \mathbf{x}_1^2$, respectively. Here, the superindices {1,2} refer to the body on which the variable is defined. Let $\bar{\mathbf{x}}^1$ and $\bar{\mathbf{x}}^2$ be the orthogonal projections of the nodes \mathbf{x}_2^2 and \mathbf{x}_2^1 onto the edges $\mathbf{x}_2^1 - \mathbf{x}_1^1$ and $\mathbf{x}_2^2 - \mathbf{x}_1^2$, respectively, as shown in Fig. 3.2. The contact segment is defined to be the *quadrilateral* specified by the points $\{\bar{\mathbf{x}}^1, \mathbf{x}_2^1, \bar{\mathbf{x}}^2, \mathbf{x}_2^2\}$. The new nodal points $\bar{\mathbf{x}}^1$ and $\bar{\mathbf{x}}^2$ are obtained as a linear combination of the form

$$\bar{\mathbf{x}}^A = (1 - \alpha^A) \mathbf{x}_1^A + \alpha^A \mathbf{x}_2^A, \quad \alpha^A \in [0, 1], \quad (A=1,2). \quad (3.2)$$

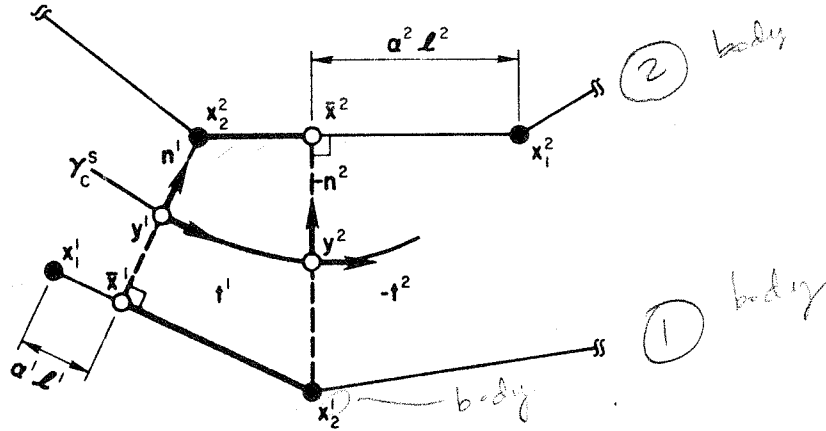


FIG.3.2 GEOMETRY ASSOCIATED WITH A TYPICAL CONTACT SEGMENT.

Expressions for the coefficients α^A may be found in Box 1. Similarly, the displacement vector at the new nodes $\bar{\mathbf{x}}^1$ and $\bar{\mathbf{x}}^2$ is given in terms of the nodal displacements \mathbf{u}_1^A and \mathbf{u}_2^A of a typical 4-node isoparametric element by

$$\bar{\mathbf{u}}^A = (1 - \alpha^A) \mathbf{u}_1^A + \alpha^A \mathbf{u}_2^A, \quad (A=1,2). \quad (3.3)$$

Relative to a typical contact segment, we introduce *tangential* and *normal* unit vectors \mathbf{t}^A and \mathbf{n}^A given for the planar case by the expressions

$$\mathbf{t}^A = \frac{\mathbf{x}_2^A - \mathbf{x}_1^A}{\|\mathbf{x}_2^A - \mathbf{x}_1^A\|}, \quad \mathbf{n}^A = \hat{\mathbf{e}}_3 \times \mathbf{t}^A, \quad (A=1,2) \quad (3.4)$$

Here, $\hat{\mathbf{e}}_3$ denotes the unit vector normal to the plane in which motion takes place. With the aid of (3.4), the gaps g_1 and g_2 at the edges of the segment are obtained according to

$$\begin{aligned} g_1 &= [\mathbf{u}_1^2 - \bar{\mathbf{u}}^1] \cdot \mathbf{n}^1 + g_0^1 \equiv [\mathbf{u}_1^2 - (1 - \alpha^1) \mathbf{u}_1^1 - \alpha^1 \mathbf{u}_2^1] \cdot \mathbf{n}^1 + g_0^1 \\ g_2 &= [\mathbf{u}_2^1 - \bar{\mathbf{u}}^2] \cdot \mathbf{n}^2 + g_0^2 \equiv [\mathbf{u}_2^1 - \alpha^2 \mathbf{u}_2^2 - (1 - \alpha^2) \mathbf{u}_1^2] \cdot \mathbf{n}^2 + g_0^2, \end{aligned} \quad (3.5)$$

where the initial gaps g_0^1 and g_0^2 are defined in terms of the initial geometry as in Box 1. Once the geometry of a typical contact segment has been defined the interpolation of the relevant quantities within the contact segment may be accomplished as follows.

BOX 1. *Definition of a Contact Segment. Planar case*

<ul style="list-style-type: none"> • Projection of a node onto the opposite element edge $\alpha^1 = \frac{(\mathbf{x}_2^1 - \mathbf{x}_1^1) \cdot (\mathbf{x}_2^2 - \mathbf{x}_1^1)}{\ \mathbf{x}_2^1 - \mathbf{x}_1^1\ ^2} \quad \alpha^2 = \frac{(\mathbf{x}_2^2 - \mathbf{x}_1^2) \cdot (\mathbf{x}_2^1 - \mathbf{x}_1^2)}{\ \mathbf{x}_2^2 - \mathbf{x}_1^2\ ^2}$ • Coordinates of the segment-nodes $\bar{\mathbf{x}}^A = (1 - \alpha^A) \mathbf{x}_1^A + \alpha^A \mathbf{x}_2^A, \quad \mathbf{x}_2^1, \mathbf{x}_2^2$ • Tangent and normal vectors $\mathbf{t}^A = \frac{\mathbf{x}_2^A - \mathbf{x}_1^A}{\ \mathbf{x}_2^A - \mathbf{x}_1^A\ } \quad \mathbf{n}^A = \mathbf{e}_3 \times \mathbf{t}^A$ • Initial gaps $g_0^1 = \ \bar{\mathbf{x}}_1^1 - \mathbf{x}_2^2\ , \quad g_0^2 = \ \mathbf{x}_2^1 - \bar{\mathbf{x}}_1^2\$
--

3.2. Interpolation within a Contact Segment. Let us first introduce an intermediate contact line parametrized within the contact segment s by $\xi \rightarrow \boldsymbol{\gamma}_s^c(\xi)$, with parameter ξ chosen for convenience as $\xi \in [0, 1]$, and such that

$$\left. \frac{d\boldsymbol{\gamma}_s^c}{d\xi}(\xi) \right|_{\xi=0} = L_s \mathbf{t}^1, \quad \left. \frac{d\boldsymbol{\gamma}_s^c}{d\xi}(\xi) \right|_{\xi=1} = L_s \mathbf{t}^2, \quad (3.6)$$

where

$$L_s \equiv \int_{\xi=0}^{\xi=1} \|d\boldsymbol{\gamma}_s^c(\xi)/d\xi\| d\xi \quad (3.7)$$

Denoting by $\mathbf{u}^A(\xi)$, $\xi \in [0, 1]$, the displacement of body Ω^A within the contact segment, the gap $g(\xi)$ is obtained according to

$$g(\xi) = [\mathbf{u}^2(\xi) - \mathbf{u}^1(\xi)] \cdot \mathbf{n}(\xi) + g_0(\xi), \quad (3.8)$$

and the "variation" of the gap given by (3.8) is computed with the aid of the directional derivative formula as

$$\delta g(\xi) \equiv [\boldsymbol{\eta}^2(\xi) - \boldsymbol{\eta}^1(\xi)] \cdot \mathbf{n}(\xi) \quad (3.9)$$

Nothing has been said so far about the explicit construction of the contact line $\xi \rightarrow \boldsymbol{\gamma}_s^c(\xi)$. Since its derivatives are specified by (3.6), one may interpolate this curve by Hermite polynomials once the position of its end points at $\xi = 0$ and $\xi = 1$ has been selected. That is, set

$$\mathbf{y}^1 \equiv (1 - \beta) \bar{\mathbf{x}}^1 + \beta \mathbf{x}_2^2, \quad \mathbf{y}^2 \equiv (1 - \beta) \mathbf{x}_2^1 + \beta \bar{\mathbf{x}}^2, \quad (3.10)$$

where $\beta \in [0, 1]$, is a pre-specified parameter. The limiting choices of $\beta = 0, 1$ correspond to selecting one of the two surfaces in contact as interpolated surface. The selection of the appropriate β should be made on the basis of the relative stiffnesses of the bodies in contact. Introducing the notation $\tilde{L}_s \equiv \|\mathbf{y}^2 - \mathbf{y}^1\|$, $\xi \rightarrow \boldsymbol{\gamma}_s^c(\xi)$ may be defined by the interpolation

$$\boldsymbol{\gamma}_s^c(\xi) \equiv \sum_{A=1}^2 v_A(\xi) \mathbf{y}^A + \tilde{L}_s \sum_{A=1}^2 \theta_A(\xi) \mathbf{t}^A, \quad (3.11a)$$

where $\{v_1, v_2, \theta_1, \theta_2\}$ are the classical Hermite polynomials given by

$$\begin{aligned} v_1(\xi) &\equiv 1 - 3\xi^2 + 2\xi^3 & v_2(\xi) &\equiv 3\xi^2 - 2\xi^3 \\ \theta_1(\xi) &\equiv \xi(1 - \xi)^2 & \theta_2(\xi) &\equiv \xi^2(1 - \xi) \end{aligned} \quad (3.11b)$$


Note that by evaluating the integral (3.7) with the aid of the trapezoidal rule we obtain $L_s = \tilde{L}_s \equiv \|y^2 - y^1\|$. In the next section, it will be seen that the interpolation of $\xi \rightarrow \gamma_s^c(\xi)$ is not explicitly needed in the final form of the finite element approximation since the integrals over the segment are approximated by the trapezoidal rule.

3.3. Finite Element Approximation. Upon introduction of the finite element discretization (3.1), the discrete version of the variational equations (2.11) may be expressed as

$$\begin{aligned} G_1 &\approx \sum_{e=1}^{E_{total}} G^e + \sum_{s=1}^{S_{total}} \int_{\gamma_s^c} \lambda_s [\eta^2 - \eta^1] \cdot \mathbf{n} \, d\Gamma = 0 \\ G_2 &\approx \sum_{s=1}^{S_{total}} \int_{\gamma_s^c} q_s \left[-\frac{\lambda_s}{\epsilon} + (\mathbf{u}^2 - \mathbf{u}^1) \cdot \mathbf{n} \right] d\Gamma = 0 \end{aligned} \quad (3.12)$$

$\int_{\gamma_s^c} \lambda_s g(\xi) \left\| \frac{d\gamma}{d\xi} \right\| d\xi$
 $\lambda_s \left(\frac{g_2(\xi) + g_1(\xi)}{2} \right) L_s$
 $\int_{\gamma_s^c} q_s g(\xi) \left\| \frac{d\gamma}{d\xi} \right\| d\xi$

Here, E_{total} refers to the total number of elements in the discretization, S_{total} refers to the total number of contact segments in the slidelines, and G^e denotes the restriction of G_1 to an element e . For the 4-node isoparametric element the displacement field is approximated according to the standard C^0 interpolation

$$\mathbf{u}^A(\mathbf{x}) \Big|_{\Omega_e^A} = \sum_{I=1}^4 N_I^A(\mathbf{x}) \mathbf{u}_I^A, \quad (A=1,2), \quad (3.13)$$


where $N_I^A(\mathbf{x})$ are the shape function for the element Ω_e^A of body Ω^A . Such an interpolation leads to well known expressions for the element stiffness matrix and residual force vector (e.g., see [19]).

The essential point in the present development pertains to the approximation within a typical contact segment of the contact pressure λ_s . In the context of the linear approximation for the displacement field, our fundamental assumption is that *the contact pressure is constant within the contact segment; i.e.,*

$$\lambda_s \equiv \lambda(\mathbf{x}) \Big|_{\gamma_s^c} = \text{CONSTANT}. \quad (3.14)$$

Since no derivatives of λ appear in (2.11a,b) no inter-segment continuity needs to be enforced on λ_s . Accordingly, the discrete equation (3.12)₂ reduces to

$$G_2^s \equiv \int_{\gamma_s^c} q_s \left[-\frac{\lambda_s}{\epsilon} + (\mathbf{u}^2 - \mathbf{u}^1) \cdot \mathbf{n} \right] d\Gamma = 0, \quad \text{for any } s \in \{1, \dots, S_{total}\}. \quad (3.15)$$

Therefore, as a result of the approximation (3.14), the contact pressure within a typical segment is given by the integral expression

$$\lambda_s = \frac{\epsilon}{L_s} \int_{\gamma_s^c} (\mathbf{u}^2 - \mathbf{u}^1) \cdot \mathbf{n} \, d\Gamma \equiv \frac{\epsilon}{L_s} \int_{\xi=0}^1 g(\xi) \left\| d\gamma_s^c(\xi) / d\xi \right\| d\xi, \quad (3.16)$$

$\frac{\epsilon (g_2(\xi) L_s + g_1(\xi) L_s)}{2 L_s}$

where the gap function $g(\xi)$ is given by (3.8). Our final approximation is concerned with the way in which (3.16) is computed. By evaluating (3.16) with the aid of the *trapezoidal* rule the final result takes the simple form

$$\lambda_s = \frac{\epsilon}{2} (g_1 + g_2) \equiv \epsilon \bar{g}_s, \quad (3.17)$$

where g_1 and g_2 are the gaps at the edges of the segment given by (3.5). It then follows from (3.17) that within a contact segment the contact pressure is *constant* and proportional to the *average gap* \bar{g}_s . By evaluating the integral terms over γ_s^ξ appearing in (3.12)₁ with the aid of the trapezoidal rule, the discrete variational equations (3.12) take the final form

$$G_1 \approx \sum_{e=1}^{E_{total}} G^e + \sum_{s=1}^{S_{total}} \lambda_s \left[\sum_{l=1}^4 \boldsymbol{\eta}_l \cdot \mathbf{c}^l \right] = 0 \quad (3.18a)$$

$$G_2^s \approx -\frac{\lambda_s}{\epsilon} + \sum_{l=1}^4 \mathbf{c}^l \cdot \mathbf{u}_l = 0, \quad \text{for any } s \in \{1, \dots, S_{total}\}, \quad (3.18b)$$

where the expressions for the residual *contact forces* have been summarized for convenience in Box 2. Equations (3.17) and (3.18) complete the proposed finite element approximation based on the perturbed Lagrangian formulation (2.11) for the contact problem.

BOX 2. Contact Surface: Finite Element Approximation

- Approximation of average gap \bar{g}_s by trapezoidal rule

$$\bar{g}_s = \frac{1}{2}(g_1 + g_2)$$
- Residual Forces due to contact

$$G_C \Big|_{\gamma_s^\xi} \equiv -\epsilon L_s \bar{g}_s \sum_{l=1}^4 \boldsymbol{\eta}_l \cdot \mathbf{c}^l$$
- where

$$\mathbf{c}_1^s \equiv -\frac{1}{2}(1-\alpha^1) \mathbf{n}^1 \quad \mathbf{c}_2^s \equiv -\frac{1}{2}(\mathbf{n}^2 + \alpha^1 \mathbf{n}^1)$$

$$\mathbf{c}_3^s \equiv \frac{1}{2}(\mathbf{n}^1 + \alpha^2 \mathbf{n}^2) \quad \mathbf{c}_4^s \equiv \frac{1}{2}(1-\alpha^2) \mathbf{n}^2$$
- Tangent Stiffness due to Contact

$$DG_2 \Big|_{\gamma_s^\xi} \cdot \Delta \mathbf{u} = \epsilon L_s \sum_{l=1}^4 \sum_{j=1}^4 \boldsymbol{\eta}_l \cdot [\mathbf{K}_{lj}^s \Delta \mathbf{u}_j]$$
- where $\mathbf{K}_{lj}^s = \mathbf{c}_l^s \otimes \mathbf{c}_j^s$

4. Penalty Procedure via Perturbed Lagrangian.

To discuss the penalty solution procedure for the nonlinear system arising from (3.18a,b), it is convenient to rephrase this problem in matrix notation as

$$G_1 \equiv \boldsymbol{\eta}^T [\mathbf{G} + \mathbf{C} \boldsymbol{\lambda}] = 0 \quad (4.1a)$$

$$G_2 \equiv \mathbf{q}^T \left[-\frac{\boldsymbol{\lambda}}{\epsilon} + \mathbf{C}^T \mathbf{u} \right] = 0 \quad (4.1b)$$

where

$$\boldsymbol{\eta}^T = [\boldsymbol{\eta}_1^T, \dots, \boldsymbol{\eta}_{E_{total}}^T], \quad \mathbf{u}^T = [\mathbf{u}_1^T, \dots, \mathbf{u}_{E_{total}}^T]$$

and

$$\mathbf{q}^T = [q_1, \dots, q_{S_{total}}], \quad \boldsymbol{\lambda}^T = [\lambda_1, \dots, \lambda_{S_{total}}]. \quad (4.2)$$

Here, \mathbf{G} denotes the residual force vector for the unconstrained problem obtained from the element contributions by the standard assembly procedure. In addition, \mathbf{C} is a $(S_{total} \times E_{total} \cdot n)$ matrix, where n is the spatial dimension of the problem, which expresses globally the local contact conditions, and is obtained by assembly of the vectors \mathbf{c}_f .

A penalty procedure may now be recovered from equations (4.1a,b) by exploiting the partitioned structure of this system and eliminating the Lagrange parameters at the *local level*. Solving for λ_s from equation (4.1b) and substituting back into (4.1a) yields the following nonlinear reduced system

$$\boldsymbol{\eta}^T [\mathbf{G} + \epsilon (\mathbf{C}\mathbf{C}^T) \mathbf{u}] = \mathbf{0} \quad (4.3)$$

Eq. (4.3) has a structure which typically arises in the treatment of the contact problem by the "pure" penalty method. It should be carefully noted, however, that in the perturbed Lagrangian formulation employed here leading to equation (4.3), the contact condition is enforced in an average sense over the contact segment. This is reflected in the use of the average gap \bar{g}_s , defined by (3.17) and results in an expression for the matrix \mathbf{C} different from the one corresponding to a standard penalty approach [5]. The reduced nonlinear system (4.3) may now be solved with the aid of Newton's method leading to the algorithm summarized, for convenience, in Box 3.

BOX 3. Penalty Iteration.

- Update displacements

$$\mathbf{u}^{(k+1)} = \mathbf{u}^{(k)} - [\mathbf{K} + \epsilon \mathbf{C}^{(k)} (\mathbf{C}^{(k)})^T]^{-1} [\mathbf{G}^{(k)} + \mathbf{C}^{(k)} \boldsymbol{\lambda}^{(k)}]$$
- Check for penetration

$$\bar{\mathbf{g}}^{(k+1)} = [\mathbf{C}^{(k+1)}]^T \mathbf{u}^{(k+1)}$$
- Update Lagrange Multipliers

$$\boldsymbol{\lambda}^{(k+1)} = \epsilon \bar{\mathbf{g}}^{(k+1)}$$

It is a well known that as the penalty parameter $\epsilon \rightarrow \infty$ the condition number of the tangent matrix for the penalty method tends to infinity. Thus, the crucial step in the penalty iteration procedure is the selection of the penalty parameter ϵ . This choice is discussed at length in the optimization literature [13,14]. In the context of finite elements procedures applied to structural problems the optimal choice for the penalty has been discussed in e.g. [9,10] and recently for contact problems in [12]. Useful guidelines for a selection of the penalty parameter in practical situation are also contained in [5]. To some extent, the intrinsic difficulties associated with the penalty iteration procedure can be circumvented by the augmented Lagrangian iteration. These and related topics are discussed in [7].

Remark 4.1. In the actual implementation of the penalty iteration method summarized in Box 3 the check for penetration should be performed in the initialization phase on the undeformed configuration to exclude rigid body motions. \square

Remark 4.2. In many contact problems the number of degrees of freedom in the slide-line is small compared to the total number of degrees of freedom in the discretization. In the context of linear analysis, static condensation [24] may be used to obtain a reduced system of equations that contains only the nodes of the slideline as unknowns, see e.g., [1,12]. Splitting the unknowns of the problem into two sets, one denoted by subscript c and associated with the nodes in the slidelines, and the other denoted by subscript a and containing the remaining unknowns, one obtains at an intermediate step of the Gaussian elimination process

$$[\bar{\mathbf{K}}_{cc} + \epsilon \mathbf{C}^{(k)} (\mathbf{C}^{(k)})^T] (\mathbf{u}^{(k+1)} - \mathbf{u}^{(k)}) = -[\bar{\mathbf{G}}_c + \mathbf{C}^{(k)} \boldsymbol{\lambda}^{(k)}] \quad (4.4)$$

where

$$\bar{\mathbf{K}}_{cc} = \mathbf{K}_{cc} - \mathbf{K}_{ac}^T \mathbf{K}_{aa}^{-1} \mathbf{K}_{ac}, \quad \bar{\mathbf{G}}_c = \mathbf{G}_c - \mathbf{K}_{ac}^T \mathbf{K}_{aa}^{-1} \mathbf{G}_a. \quad (4.5)$$

This small system of equations is now used in the contact iteration process. Obviously, the matrix $\bar{\mathbf{K}}_{cc}$ has to be stored to avoid recomputations which would otherwise eliminate the advantage of the static condensation procedure. \square

Remark 4.3. An alternative form of the penalty iteration for the contact problem arises by exploiting the special structure of the tangent matrix. The essential point to note is that the tangent matrix $\mathbf{K}_T^{(k)} \equiv \mathbf{K} + \epsilon \mathbf{C}^{(k)} (\mathbf{C}^{(k)})^T$ may be assembled by a sequence of *rank one* updates of the form $\mathbf{C}^{(k)} (\mathbf{C}^{(k)})^T = \sum_{s=1}^{S_{total}} (\mathbf{c}^s)^{(k)} (\mathbf{c}^s)^{(k)T}$. With the aid of the Sherman-Morrison formula for the inverse of a rank-one updated matrix, the inverse of the tangent matrix may be readily obtained as the result of the following updating procedure

$$(\mathbf{K}^s)^{-1} = (\mathbf{K}^{s-1})^{-1} - \frac{\epsilon}{1 + \epsilon (\mathbf{r}^s)^{(k)T} (\mathbf{c}^s)^{(k)}} (\mathbf{r}^s)^{(k)} (\mathbf{r}^s)^{(k)T}, \quad (s=1, \dots, S_{total}) \quad (4.6)$$

where

$$(\mathbf{r}^s)^{(k)} = \mathbf{K}^{-1} (\mathbf{c}^s)^{(k)}. \quad (4.7)$$

The advantage of this solution strategy is that the factorization of the matrix \mathbf{K} for the unconstrained problem needs to be performed only once. Note that this procedure entails the solution of the system (4.7) for each contact segment. Thus, it becomes economical only when the number of degrees of freedom in contact is small compared to the number of overall unknowns. In addition, from a practical standpoint, its application to large problems only makes sense in conjunction with the static condensation procedure discussed in Remark 4.2. It should be noted that in this procedure \mathbf{K}^s must be regular. \square

5. Numerical Examples.

In this section we compare the performance of the procedure developed in this paper with traditional penalty methods in which the contact constraint is enforced on a nodal basis. For

this purpose we consider first the indentation of a rigid punch into an elastic foundation for the case when nodes of the two bodies lying in the contact interface are not aligned. Two alternative implementations of the classical nodal penalty methods are considered which differ in the particular treatment given to the slide line. The traditional approach in which a master and a slave contact surface are defined a priori, and a symmetric treatment of the slide line employed in [5,11] in which the role of master and slave surface is sequentially interchanged. To illustrate the overall performance of the proposed procedure in a practical situation, we conclude this section with an example which involves contact of two flexible bodies and includes rate independent elasto-plastic behavior.

Rigid Punch on an Elastic Foundation. If attention is restricted to the particular case of linear kinematics, it is possible to enforce the contact conditions on a node-to-node basis. However, in the more general context of large deformations, a node-to-node treatment is no longer possible. Thus, with an eye directed towards nonlinear applications (to be considered in a forthcoming paper), we address in this example performance in the general case not restricted to node-to-node contact.

For this purpose we consider the indentation of a rigid punch with the foundation first modeled by two elements, as shown in Fig. 5.1a. The elastic properties of the foundation were taken as $E = 1.d+5$, and $\nu = 0.5$, and the penalty parameter was chosen as $\epsilon = 1.d+7$. The results obtained with the procedure advocated here and with the nodal penalty approach with single and double pass on the slide line are shown in Fig. 5.1b to Fig. 5.1d. In the present approach, use of the *average* gap \bar{g} defined by (3.15) results in the penetration profile depicted in Fig. 5.1b. This profile corresponds to an intermediate situation between the total penetration obtained with the nodal penalty approach and single pass, as shown in Fig 5.1d, and the absence of penetration obtained with the double pass technique shown in Fig 5.1c. For subsequent refinement of the mesh one obtains the profiles shown in Figs. 5.2a,b,c,d and Fig 5.3a,b,c,d. In the one pass calculation the surface of the foundation is taken as the master surface.

TABLE 1. *Nodal Penalty versus Proposed Method.*

Number of Elements		Perturbed Lagrangian	One Pass Penalty	Two Pass Penalty	Node to Node
2	v_a	1.015×10^{-2}	1.623×10^{-2}	6.623×10^{-3}	-
	v_b	1.254×10^{-2}	1.621×10^{-2}	8.882×10^{-3}	-
8	v_a	9.580×10^{-3}	8.442×10^{-3}	8.109×10^{-3}	-
	v_b	9.273×10^{-3}	6.914×10^{-3}	8.105×10^{-3}	-
32	v_a	1.089×10^{-2}	9.687×10^{-3}	9.614×10^{-3}	-
	v_b	1.089×10^{-2}	1.046×10^{-2}	9.614×10^{-3}	-
88	v_a	1.162×10^{-2}	1.256×10^{-2}	1.101×10^{-2}	1.167×10^{-2}
	v_b	1.162×10^{-2}	1.256×10^{-2}	1.101×10^{-2}	1.167×10^{-2}

The vertical displacement of the punch for increasingly refined meshes has been tabulated in Table 1 for the three approaches considered. The solution obtained in the case of node-to-node contact, for which all three approaches coincide, is also included in Table 1 for comparison purposes. The proposed procedure shows the closest agreement with the the node-to-node approach. In addition, for reference purposes we note that the exact solution for the indentation of a rigid punch on an elastic half space [17, p.73] gives the value $v_{exact} = 1.89 \cdot 10^{-2}$, obtained with the aid of Simpson's rule.

Flexible Punch on an Elastoplastic Foundation. As our final example we consider the indentation of a *flexible* punch into an *elastoplastic* foundation. Our purpose is to illustrate the performance of the proposed procedure in a more realistic situation that involves (a) general (as opposed to node-to-node) contact, (b) inelastic (nonlinear) material response and (c) two *deformable* bodies in contact.

The finite element mesh, shown in Fig. 5.4, consists of 120 bi-linear isoparametric elements. The elastoplastic response of the foundation is characterized by a pressure independent von Mises yield condition with kinematic/isotropic saturation hardening. The material properties of the model are also shown in Fig. 5.4. The mixed finite element formulation for this type of elastoplastic model is discussed in [26].

For comparison purposes the problem is first solved ignoring inelastic effects. The deformed finite element mesh and stress contours for the vertical stress corresponding to the elastic case are shown in Figs. 5.5a,b. The analogous results for the elastoplastic case are shown in Figs. 5.6a,b, and the plastic region is depicted in Fig. 5.6c. Although no closed form solution for this problem exists, a comparison between Fig 5.5b and Fig. 5.6b reveals that the vertical stresses in the plastic case are considerably mitigated below the punch, as one would expect. One should note that the mesh is not fine enough to obtain an accurate resolution of the stress. This is apparent in the contact interface.

The above results demonstrate that the proposed procedure for the analysis of contact problems is capable of handling a wide range of engineering applications. These include situations in which both bodies are flexible, with nonlinear inelastic behavior, and a general treatment of the slide line not restricted to node-to-node contact.

6. Concluding Remarks.

- (i) The mixed approximation to the perturbed Lagrangian proposed in this paper has been discussed for the particular case of a linear approximation to the displacement field and constant contact pressure over the contact segment. Related work in the context of the incompressible problem suggest higher order interpolation schemes. Typically, one may wish to consider a quadratic approximation for the displacement field in conjunction with linear contact pressure distributions over the contact segment.
- (ii) For the sake of simplicity in the presentation, attention has been restricted to the case of linear kinematics. The proposed procedure, however, is particularly useful in the finite case where node-to-node contact can no longer be assumed.

- (iii) The final solution algorithm has been formulated on the basis of a penalty procedure obtained from the mixed formulation by eliminating the contact pressure at the element level. Alternative iterative algorithms based on the use of augmented Lagrangian procedures are explored in [16].

References

- [1] Francavilla, A. and O.C. Zienkiewicz, "A Note on Numerical Computation of Elastic Contact Problems," *Int. J. Num. Meth. Engng.* Vol. 9, pp. 913-924, 1975.
- [2] S. K. Chan, and I. S. Tuba, "A Finite Element Method for Contact Problems of Solid Bodies: I. Theory and Validation," *Int. J. Mech. Sci.*, Vol. 13, pp. 627-639, 1971.
- [3] T. R. J. Hughes, R. L. Taylor, J. L. Sackman, A. Curnier, and W. Kanoknukulchai, "A Finite Element Method for a Class of Contact-Impact Problems," *Comp. Meth. Appl. Mech. Engng.*, Vol. 8, pp. 249-276, 1976.
- [4] Oden, J.T., "Exterior Penalty Methods for Contact Problems in Elasticity," in Europe-US workshop *Nonlinear Finite Element Analysis in Structural Mechanics*, Bathe, Stein and Wunderlich, Eds., Springer-Verlag, Berlin (1980).
- [5] J. O. Hallquist, "NIKE2D: An Implicit, Finite- Deformation, Finite- Element Code for Analyzing the Static and Dynamic Response of Two- Dimensional Solids," *Rept. UCRL-52678*, University of California, Lawrence Livermore National Laboratory, 1979.
- [6] N. Kikuchi, and J. T. Oden, "Contact Problems in Elastostatics," in *Finite Elements: Special Problems in Solid Mechanics*, Vol. IV, Ed. Oden and Carey, Prentice-Hall, Englewood Cliffs, N. J., 1984.
- [7] Fortin, M., and R. Glowinsky, *Augmented Lagrangian Methods*, North-Holland, Amsterdam, 1983.
- [8] Glowinski, R. & P. le Tallec, "Finite Elements in Nonlinear Incompressible Elasticity," in *Finite Elements Vol IV: Special Problems in Solid Mechanics*, Ed. Oden & Carey, Prentice Hall Inc., N.J. (1984).
- [9] C. A. Felippa, "Error Analysis of Penalty Function Techniques for Constraint Definition in Linear Algebraic Systems," *Int. J. Num. Meth. Engng.*, Vol. 11, pp. 709-728, 1977.
- [10] C. A. Felippa, "Iterative Procedures for Improving Penalty Function Solutions of Algebraic Systems," *Int. J. Num. Meth. Engng.*, Vol. 12, pp. 821-836, 1978.
- [11] Key, S.W., "HONDO II A Finite Element Computer Program for the Large deformation Dynamic Response of Axisymmetric Solids," *Report, SAND78-0422* Sandia Laboratories, Albuquerque, New Mexico, 1978.
- [12] Wriggers, P. and B. Nour-Omid, "Solution Methods for Contact Problems," *Report No UCB/SESM 84/09* Dept. Civil Engineering, University of California, Berkeley, 1984.
- [13] D. G. Luenberger, *Linear and Nonlinear Programming*, 2nd Edition, Addison-Wesley Pub. Co., Reading, Massachusetts, 1984.
- [14] Bertsekas, D.P., *Constrained Optimization and Lagrange Multiplier Methods*, Academic Press, New York, 1982.
- [15] Carey, G. F., and J.T. Oden, *Finite Elements, Volume II*, Prentice-Hall Inc., Englewood Cliffs, New Jersey, 1982.
- [16] Wriggers, P., J.C. Simo, and R. L. Taylor, "Penalty and Augmented Lagrangian Formulations for Contact Problems," *To appear*, In Proceedings of NUMETA Conference, Swan 1985.

- [17] Girkmann, K., *Flächentragwerke*, 4th ed., Springer Verlag, Vienna, 1956.
- [18] P. Wriggers, "Zur Berechnung von Stoss- und Kontaktproblemen mit Hilfe der Finite-Element Methode," *Bericht Nr. F81/1*, Forschungs- und Seminarberichte aus dem Bereich der Mechanik der Universitaet Hannover, Hannover, 1981.
- [19] O. C. Zienkiewicz, *The Finite Element Method*, 3rd Edition, McGraw-Hill, London, 1977.
- [20] Valliappan, S., I.K. Lee, and P. Boonlualohr, "Non-linear Analysis of Contact Problems," in *Numerical Methods in Coupled Systems*, R.W. Lewis, P. Bettess, E. Hinton Edts., John Wiley & Sons., 1984.
- [21] Kikuchi, N., "A Class of Rigid Punch Problems involving Forces and Moments by Reciprocal Variational Inequalities," *J. Struct. Mech.*, Vol. 7, pp.273-295, 1979.
- [22] Oden, J.T., N. Kikuchi and Y.J. Song, "Penalty-Finite Element Methods for the Analysis of Stokesian Flows," *Comp. Meth. Appl. Mech. Engng.*, 31, pp. 297-322.
- [23] Marsden, J.E., and T.J.R. Hughes, *Mathematical Foundations of Elasticity*, Prentice-Hall, Inc., Englewood Cliffs, New Jersey, 1983.
- [24] Wilson, E., "The Static Condensation Algorithm," *Int. J. Num. Meth. Engng.*, Vol. 8, pp. 199-203, 1974.
- [25] Reddy, J.N., "On Penalty Function Methods in the Finite Element Analysis of Flow Problems," *Int. J. Num. Meth. Fluids.*, Vol. 2, pp. 151-172, 1984.
- [26] Simo, J.C. and R.L. Taylor, "Consistent Tangent Operators for Rate-Independent Elastoplasticity," *Comp. Meth. Appl. Mech. Engng.*, To appear.

Figure Captions.

Figure 3.1. Discretization of the contact interface.

Figure 3.2. Geometry of a typical *contact segment*.

Figure 5.1. Rigid punch problem. 3-element mesh.

- (a) Finite element mesh
- (b) Proposed procedure based on perturbed Lagrangian formulation.
- (c) Penalty formulation with symmetric (2-pass) treatment of the slide line.
- (d) Penalty formulation with traditional (1-pass) treatment of the slide line.

Figure 5.2. Rigid punch problem. 11-element mesh.

- (a) Finite element mesh.
- (b) Proposed procedure based on perturbed Lagrangian formulation.
- (c) Penalty formulation with symmetric (2-pass) treatment of the slide line.
- (d) Penalty formulation with traditional (1-pass) treatment of the slide line.

Figure 5.3. Rigid punch on elastic foundation. 69-element mesh.

- (a) Finite element mesh.
- (b) Proposed procedure based on perturbed Lagrangian formulation.
- (c) Penalty formulation with symmetric (2-pass) treatment of the slide line.
- (d) Penalty formulation with traditional (1-pass) treatment of the slide line.

Figure 5.4. Indentation of a *Flexible* punch on an *elastoplastic* foundation. Finite element mesh. 120-linear isoparametric elements.

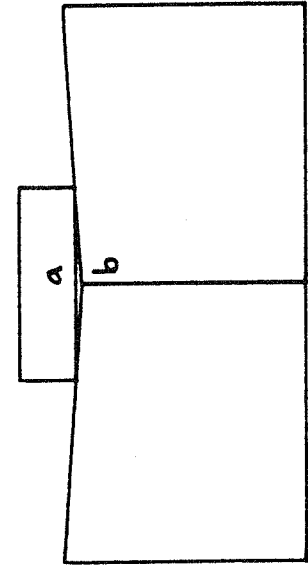
Figure 5.5a. Indentation of a flexible punch. Deformed finite element mesh for the case of an *elastic* foundation.

Figure 5.5b Indentation of a flexible punch. Stress contours of the vertical stress σ_{yy} for the case of *elastic* response of the foundation.

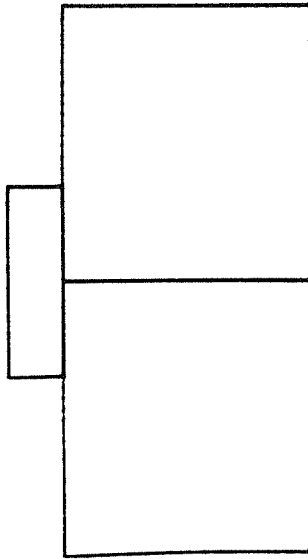
Figure 5.6a. Indentation of a flexible punch. Deformed finite element mesh for the case of *elasto-plastic* response of the foundation.

Figure 5.6b. Indentation of a flexible punch. Stress contours of the vertical stress σ_{yy} for the case of *elastoplastic* response of the foundation.

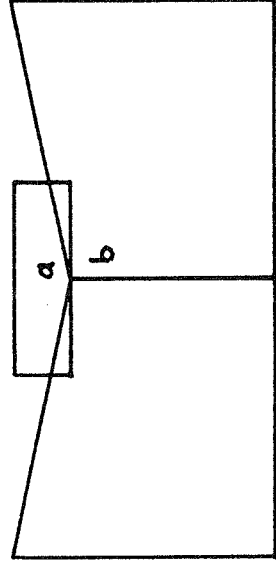
Figure 5.6c. Indentation of a flexible punch. *Elastoplastic* response of the foundation: yield surface.



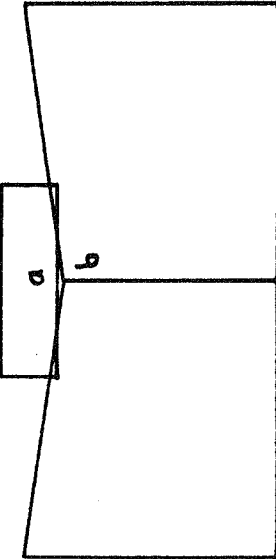
(a)



(b)

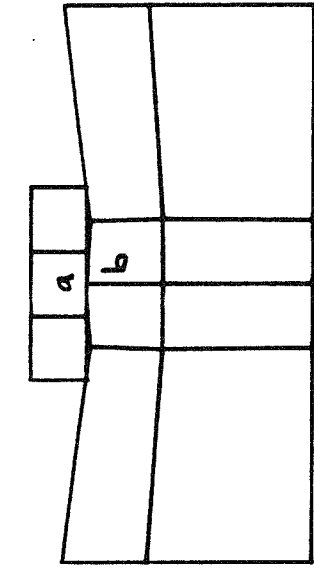


(c)

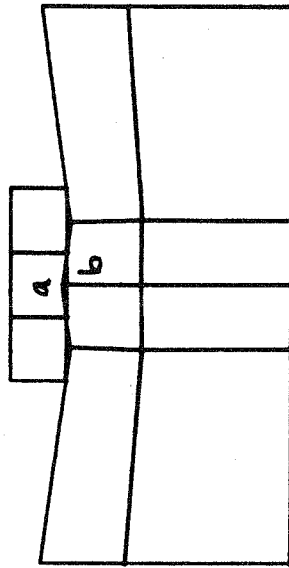


(d)

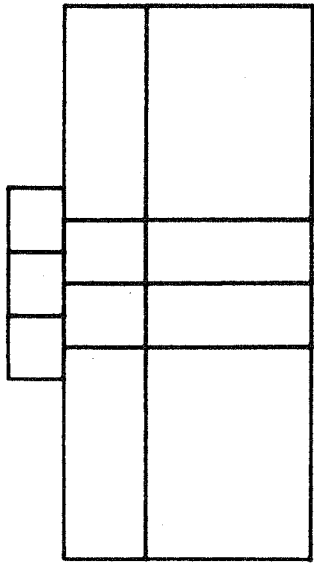
Figure 5.1. Rigid punch problem. 3-element mesh.
 (a) Finite element mesh
 (b) Proposed procedure based on perturbed Lagrangian formulation.
 (c) Penalty formulation with symmetric (2-pass) treatment of the slide line.
 (d) Penalty formulation with traditional (1-pass) treatment of the slide line.



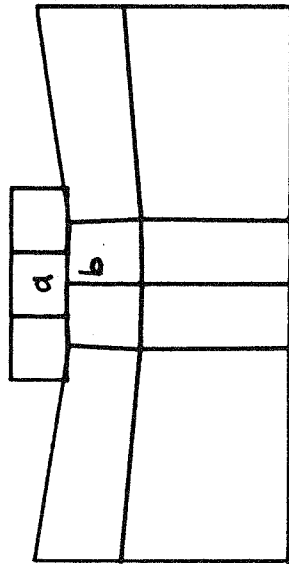
(a)



(b)

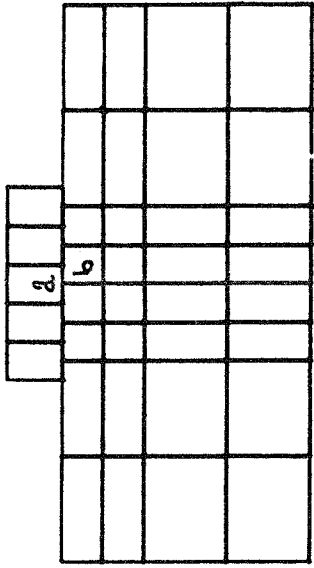


(c)

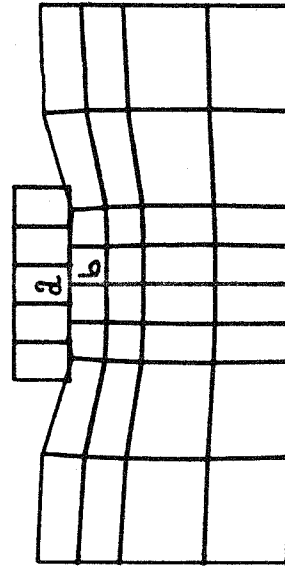


(d)

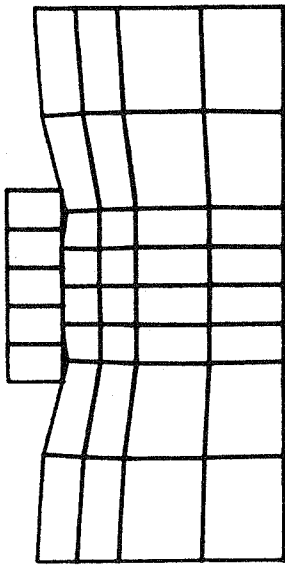
Figure 5.2. Rigid punch problem. 11-element mesh.
 (a) Finite element mesh.
 (b) Proposed procedure based on perturbed Lagrangian formulation.
 (c) Penalty formulation with symmetric (2-pass) treatment of the slide line.
 (d) Penalty formulation with traditional (one-pass) treatment of the slide line.



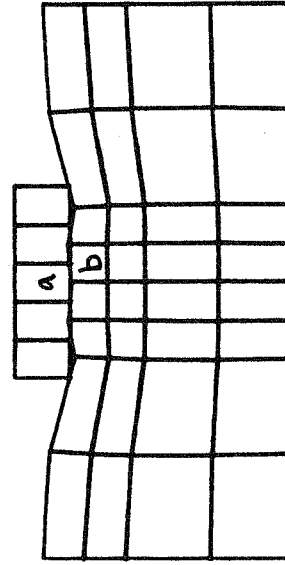
(a)



(b)



(c)



(d)

Figure 5.3. Rigid punch on elastic foundation. 69-element mesh.

(a) Finite element mesh.

(b) Proposed procedure based on perturbed Lagrangian formulation.

(c) Penalty formulation with symmetric (2-pass) treatment of the slide line.

(d) Penalty formulation with traditional (one-pass) treatment of the slide line.

Elastoplastic Foundation: Material Properties.

<i>Bulk Modulus (K)</i>	8000.00
<i>Shear Modulus (G)</i>	5000.00
<i>Yield Stress (σ_y)</i>	5.00
<i>Linear Hardening (H)</i>	100.00

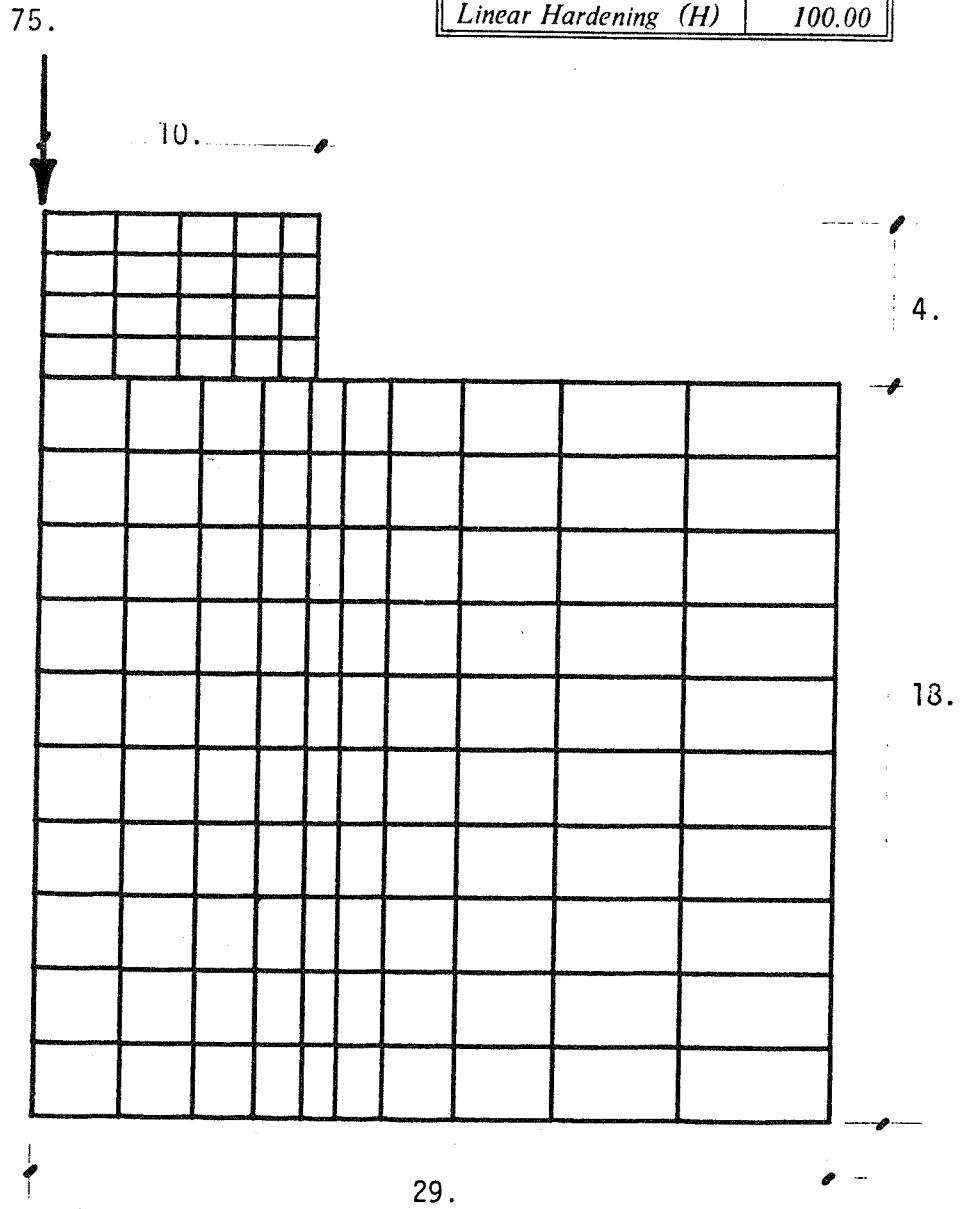


Figure 5.4. Indentation of a *Flexible* rigid punch on an *elastoplastic* foundation. Finite element mesh. 120-linear isoparametric elements.

SCALE 50 : 1

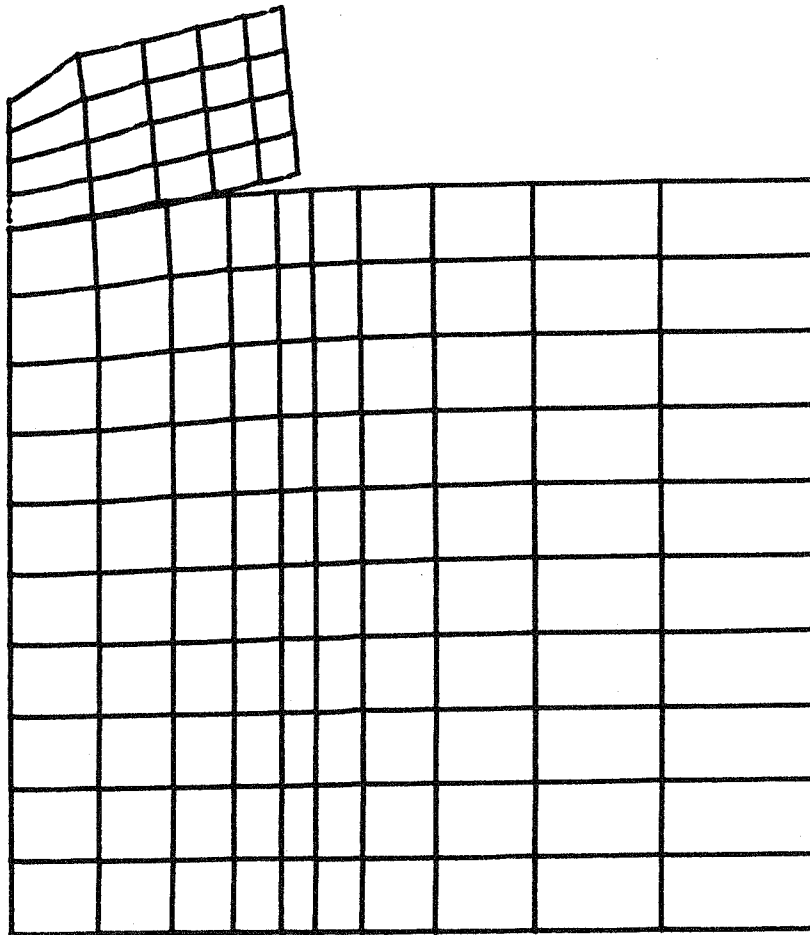


Figure 5.5a. Deformed finite element mesh for the case of an *elastic* foundation.

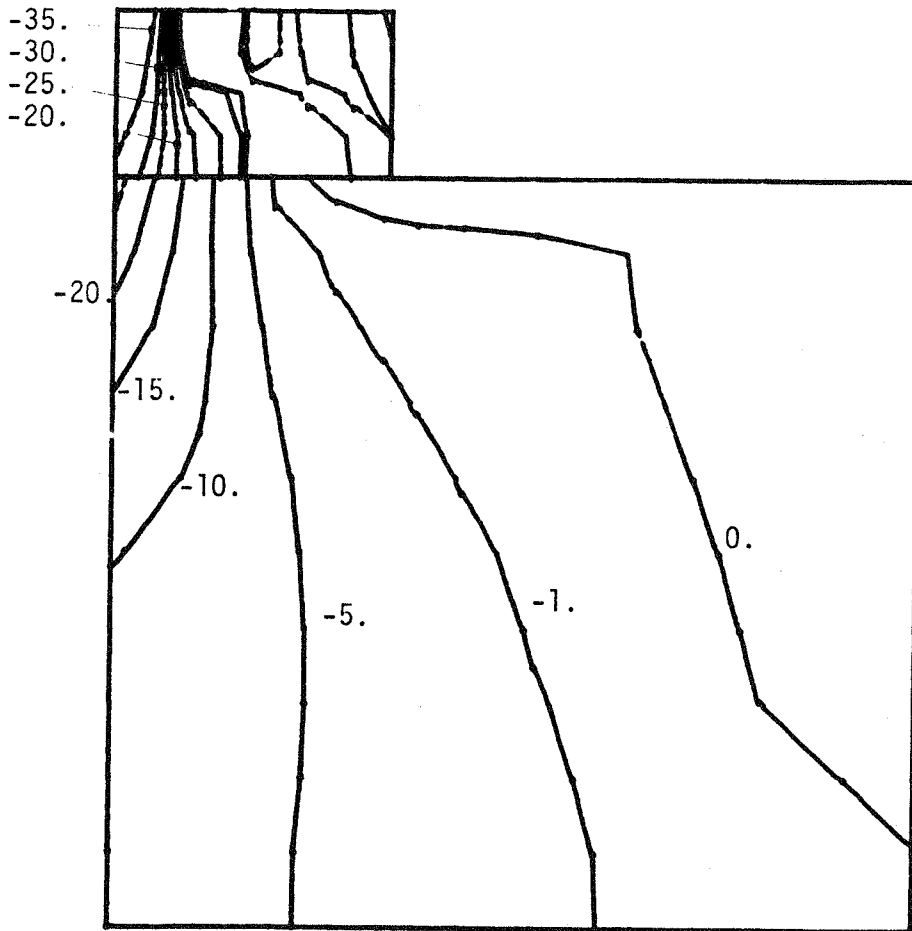


Figure 5.5b Stress contours of the vertical stress σ_{yy} for the case of *elastic* response of the foundation.

SCALE 50 : 1

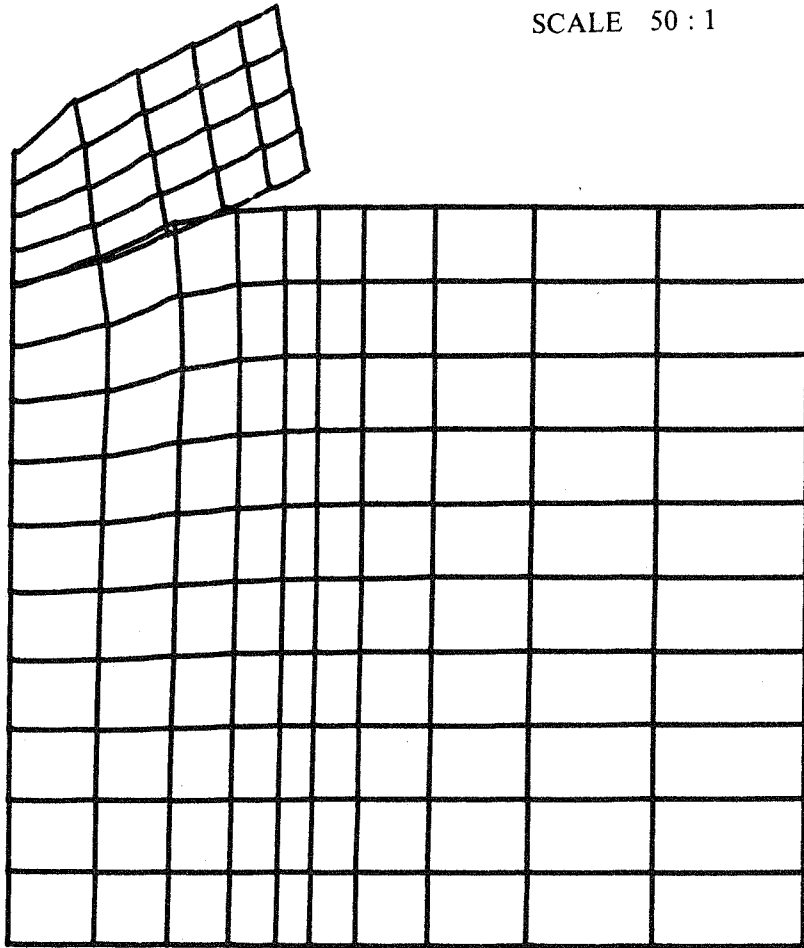


Figure 5.6a. Deformed finite element mesh for the case of *elasto-plastic* response of the foundation.

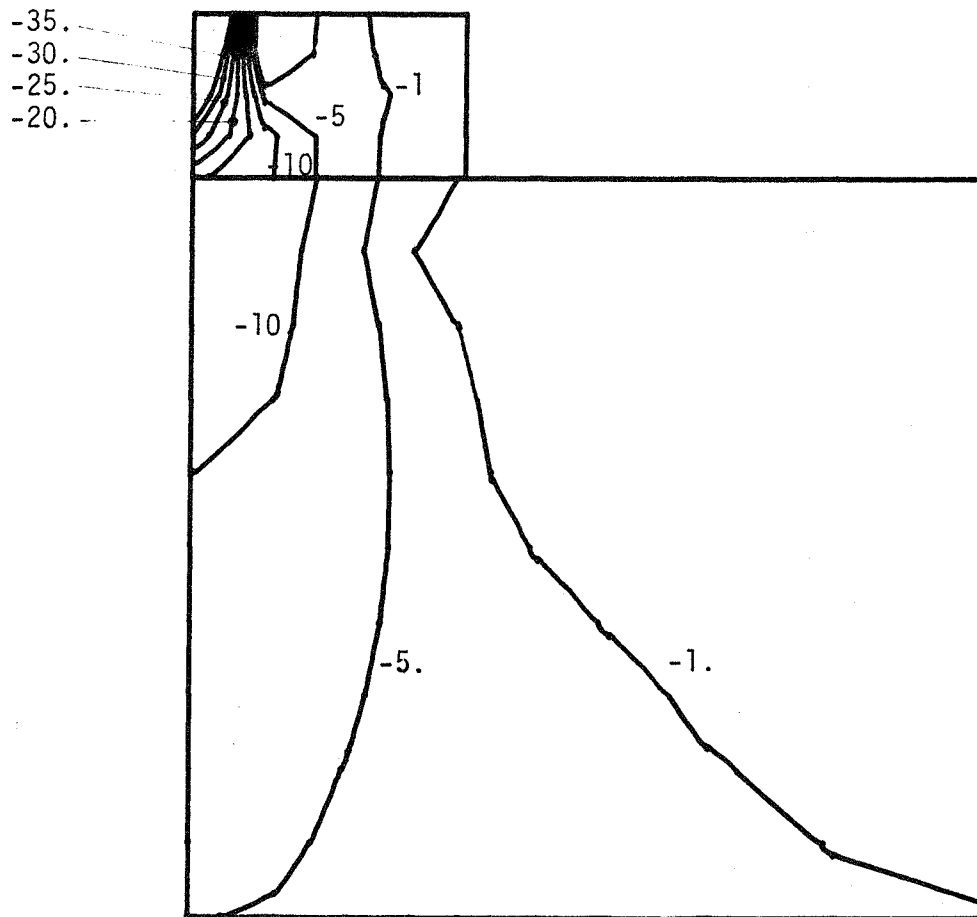


Figure 5.6b. Stress contours of the vertical stress σ_{yy} for the case of *elastoplastic* response of the foundation.